Iranian Journal of Science and Technology, Transactions of Civil Engineering (2022) 46:2677–2695
https://doi.org/10.1007/s40996-021-00652-5

TECHNICAL NOTE

Mechanical Properties of Hybrid Self-Compacting Fibre-Reinforced Concrete (SCC-FRC) Containing PVA and PP Fibres

Sadaqat Ullah Khan[1] · **Tehmina Ayub**[2]

Received: 6 February 2021 / Accepted: 25 April 2021 / Published online: 27 May 2021

Abstract
Concrete is a widely used building material, which is good in compression, but weak in tension. The poor tension properties of concrete are covered by using steel bars as reinforcement, which enable concrete to withstand almost all types of loads and provide ductility to structural members. However, it has some drawbacks, such as controlling multi-level cracking. It is widely accepted that using the different forms of fibres together is the only way to achieve strength, ductility, and resilience to control multi-level cracking of reinforced concrete. The novelty of this study is the development of the hybrid self-compacting fibre-reinforced concrete (SCC-FRC) with polyvinyl alcohol (PVA) and polypropylene (PP) fibres to eliminate the problems associated with steel fibres. This hybrid FRC can provide better crack controlling at all stages and enhancement in mechanical properties. Out of 14 mixes, one SCC mix (without fibres) served as a control mix. The rest SCC-FRC mix contained only 2% volume fraction of PVA fibres, 2% volume fraction of monofilament PP fibres, and 2% volume fraction fibrillated PP fibres of lengths 13, 19, and 25 mm, respectively, served as the benchmark for the hybrid mixes. The remaining six SCC-FRC mixes were hybrid and consisted of 1.5 and 0.5% volume fractions of PVA and PP fibres, respectively. Out of the six mixes, three included monofilament fibres measuring 13, 19, and 25 mm in length, while the other three had fibrillated fibres measuring 13, 19, and 25 mm in length. The fresh and hardened state properties of all mixes were determined by following EFNARC and ASTM standards. The hardened properties were determined by testing the specimens in compression, split tension, flexure, and direct tension. The test results showed that PVA and PP fibres as a hybrid significantly improved strength, ductility, and crack arrest.

Keywords Hybrid · SCC · FRC · PVA fibres · Monofilament and fibrillated polypropylene (PP) fibres

1 Introduction

Since the beginning of the twenty-first century, the emphasis is on smart materials that can meet the demand and economy and require lesser maintenance. In this respect, macro- and microfibres as hybrid fibre-reinforced concrete can be one of the solutions. Many hybrid FRC using steel and PP fibres has been successfully achieved in early research. Researchers are now driving research to investigate fibres other than steel fibres to minimise the cost. Therefore, the significance of this research was to identify the correct type and content of PVA and PP fibres that can satisfy the crack controlling at all stages and enhancement in mechanical properties. The use of PVA fibres is less costly than steel fibres, and it has no drawbacks such as high weight-to-volume ratio, corrosion, and high thermal conductivity. Thus, sustainability and durability are eventually the objectives of this study.

Concrete is the most in abundance used material in the world after water. Due to good compressive behaviour, it is a widely used building material, while poor tension properties are covered using steel bars as reinforcement. Although steel bars enable concrete to withstand almost all types of loads and provide ductility to structural members, it has some drawbacks such as controlling cracks and penetration of ingress substances that may cause corrosion of steel (Shi et al. 2020). The scattered fibre reinforcement provides

✉ Sadaqat Ullah Khan
sadaqat@neduet.edu.pk

Tehmina Ayub
tehmina@neduet.edu.pk

[1] Department of Urban and Infrastructure Engineering, NED University of Engineering and Technology, Karachi, Pakistan

[2] Department of Civil Engineering, NED University of Engineering and Technology, Karachi, Pakistan

additional reinforcement to bridges the crack for stress transfer to overcome these issues (Chen and Qiao 2011). The flexural and post-cracking performance of concrete can be improved by adding fibres to the concrete matrix to strengthen the crack arrestment ability of concrete. Over the past few decades, FRC has been widely used in numerous applications, such as grade slabs (Alani and Beckett 2013), tunnel linings (Kaufmann et al. 2013), and precast components (Peyvandi et al. 2013).

The ACI Committee categorises fibres into glass, steel, synthetic, and natural fibres (Shah et al. 1993), and each category has been explored in several studies (Azevedo et al. 2021; Zeyad et al. 2020; Yildizel et al. 2020; Al-Attar et al. 2020; Haido et al. 2021; Abdul-Rahman et al. 2020). Steel fibres are the most common type in both research and practical applications owing to their high efficiency. However, there are problems with steel fibres, such as a significant reduction in workability, easy rusting, and basseting (Balouch et al. 2010). There are also weaknesses in glass, synthetic, and natural fibres, including poor alkaline resistance (Xiaochun et al. 2017), relatively weak mechanical properties, and long-term performance uncertainty. Fibres are divided into three groups according to their size: microfibres, macrofibres, and mesofibres (Khan et al. 2020). Generally, microfibres are tens of microns in diameter and 6–20 mm in length. These were commonly accepted as an important way of managing plastic shrinkage. However, they give slight structural benefits for concrete if structures reach the large-deformation zone because microfibres are small. Besides, macrofibres, usually 30–60 mm long and more than 0.3 mm in diameter, can bear loads and bridging cracks after concrete matrix breaks similar to steel bar reinforcement (Shi et al. 2020; Etli et al. 2018). Mesofibres, on the other hand, are smaller than macrofibres but larger than microfibres and are capable of bridging the cracks from the micro level to the macro level up to some extent (Khan et al. 2020). Since no single form of fibre can provide strength, ductility, and resilience at all loading stages, combining various fibre sizes is required to control multi-level cracking of reinforced concrete (Soe et al. 2013; Kim et al. 2011; Tian et al. 2015).

Sivakumar and Santhanam (2007) reported that high-strength FRC with PP and steel fibres performed better than other combinations of hybrid fibres, such as polyester steel fibres and glass steel fibres, in all respects. The mechanical properties of reinforced concrete with hybrid fibres, including micro-PP fibres and different kinds of steel fibres, have been studied by Qian and Stroeven (2000). It was reported that the short steel fibres (6 mm) improved the compressive strength more effectively than the tensile strength of concrete, while the big ones (30 and 40 mm) improved the post-cracking strength of the hybrid fibre matrix in particular. The optimum concentration of micro-PP fibres was also found in the hybrid fibre matrix at around 0.15%. Afroughsabet and Ozbakkaloglu (2015) investigated concrete with steel and PP fibres and found that hybrid FRC is more advantages of high cracking strength and improved post-cracking toughness as compared to steel fibre-reinforced concrete. Previous studies (Song et al. 2005; Tabatabaeian et al. 2017) have published similar results and reported that hybrid use of long steel fibres and long macro-PP fibres had improved the post-peak response of hybrid FRC.

Hsie et al. (2008) determined the efficiency of hybrid FRC with 12–25-mm micro-PP fibres (0.1% fraction) and 60-mm macro-PP fibres (0.3–1% fraction). It was found that the mechanical properties and post-cracking strength of hybrid FRC were higher than single fibre-reinforced concrete (Hsie et al. 2008). The standard shape of steel fibres (crimped, hooked end, and straight) investigated (KM, Af, and Varghese, S, 2014; Li et al. 2018) using a fixed aspect ratio of PP fibres. Asok and George (2016) performed a study on the mechanical properties of hybrid steel–PP fibre concrete using 1% and 0.035% volume fractions of hooked end steel and monofilament PP fibres. The results showed that the compressive, tensile splitting and flexural strengths of hybrid steel–PP FRC were obtained higher than the plain concrete. Sukontasukkul (2004) investigated the tensile response of FRC containing steel and PP fibres as alone and as a hybrid system by utilising 1 to 5% volume fractions. The outcome of the study (Sukontasukkul 2004) revealed that the behaviour of FRC using steel fibres was typical, i.e. the peak of the load occurred at a minimal deformation, and was shadowed by the fall of the load to zero without any sign of the load recovery. Furthermore, the behaviour of FRC-incorporating PP fibres was more ductile as compared to the steel fibres alone. It showed a typical double-peak response, i.e. the first peak occurred at a small deformation and the second peak occurred at a large deformation.

Polyvinyl alcohol (PVA) is an organic fibre explored 50 years ago by the Japanese; however, it is used as reinforcing fibres since the 1980s. PVA fibres have a higher Young's modulus compared to conventional concrete or cement mortar, as shown in Table 1. PVA fibres offer better results in terms of mechanical properties in engineered cementitious composites (ECC) without coarse aggregates (Li 2008), as well as in concrete (Nuruddin et al. (2014); Holschemacher and Höer 2008a). The use of PVA fibres in the reinforced concrete (RC) column exposed to elevated temperature was also found better than the RC column without PVA fibres in ductility and energy absorption (Said et al. 2020). Also, the use of a 2% volume fraction of PVA fibres exhibited the strain-hardening response (Nuruddin et al. 2014; Holschemacher and Höer 2008a).

This overview presents the extent of investigations performed to date using a hybrid combination of steel and PP fibres. PP fibre is less effective than steel fibres due to lower elastic modulus (Shi et al. 2020). On the other hand, the

Table 1 Physical and chemical properties of cement and fly ash

	Cement	Fly ash
Appearance	Fine-grained dry powder	Fine-grained dry powder
Colour	Grey	Light grey
Specific gravity	3.05	2.3
Fineness	Less than 45 micron	< 25% retained on 45-micron sieve
Particle shape		Spherical
Chemical properties (%)		
Calcium oxide (CaO)	62.13	7.80
Silica (SiO_2)	20.85	37.60
Alumina (Al_2O_3)	4.77	26.33
Iron oxide (Fe_2O_3)	3.51	4.40
Magnesium oxide (MgO)	1.43	1.81
Sulphur trioxide (SO_3)	1.88	0.47
Chloride (Cl)	–	0.031
Alkali Eq	–	0.89
Loss on ignition (LOI)	1.15	4.05
Water soluble phosphate (P_2O_5)	–	0.02
Manganese oxide (MnO)	–	0.038
Phosphorus oxide (P_2O_5)	–	1.16
Potassium oxide (K_2O)	–	0.68
Sodium oxide (Na_2O)	–	0.44
Titanium oxide (TiO_2)	–	1.13
Free CaO	–	0.20
Moisture		12.95

use of steel fibres also has concerns such as higher thermal conductivity (Corinaldesi and Moriconi 2012), low fire resistance (Empelmann et al. 2008), injuries caused during the production of steel fibres, tire puncture hazards in pavements, and corrosion of fibre close to the concrete surface (Granju and Balouch 2005). Thus, there is a need to investigate the combination of PP fibres with macrofibres other than steel. The novelty of this study is the development of the hybrid FRC with PVA and PP fibres to eliminate the problems associated with steel fibres. This hybrid FRC can provide better crack controlling at all stages and enhancement in mechanical properties.

The present study aims to investigate the behaviour of hybrid SCC-FRC reinforced with PVA and PP fibres in the fresh and hardened state subjected to compression, direct and indirect tension, along flexure. Two types of PP fibres, typically known as "monofilament" and "fibrillated", were intended to investigate together with PVA fibres to assess hybrid SCC-FRC's behaviour. PVA as macrofibres and monofilament and fibrillated PP as microfibres were used. A total of 2% volume fraction comprised of 1.5% volume of PVA and 0.5% volume fraction of monofilament or fibrillated PP fibres was used in hybrid SCC-FRC. The hybrid SCC-FRC mixes are compared with the control mix without fibres. Hybrid mixes are also compared with the mixes containing PVA fibres, PP monofilament, or PP fibrillated fibres alone.

2 Materials and Experimental Programme

All mixes contained ASTM Type I ordinary Portland cement (OPC) and Class F Fly ash meeting ASTM C618 standard (37ASTM C 618(2000), "Standard Specification for Coal Fly Ash and Raw or Calcined Natural Pozzolan for Use as a Mineral Admixture in Concrete", ASTM International 2000). The OPC and Fly ash were used as 70 and 30% by weight, respectively. Table 1 shows their physical and chemical properties, and fly ash qualifies the requirement of class F as per ASTM C618 standard (37ASTM C 618(2000), "Standard Specification for Coal Fly Ash and Raw or Calcined Natural Pozzolan for Use as a Mineral Admixture in Concrete", ASTM International 2000). Use Fly Ash also improves concrete workability with limited use of the viscosity-modifying agent (VMA).

The fine aggregate in this study was river sand that passed through a 4.75-mm sieve, while the coarse aggregate was gravel that passed through a 12-mm sieve and was retained on 4.75-mm sieves. Three fibre types, i.e. PVA fibres (having a length of 30 mm), monofilament PP fibres (having lengths of 13 19, and 25 mm), and fibrillated PP fibres (having lengths of 13, 19, and 25 mm), were used. Monofilament and fibrillated PP fibres were used with the PVA fibres as a hybrid to assess SCC performance. The shapes and properties of all fibres are shown in Fig. 1 and Table 2. The fibrillated PP and PVA fibres are relatively hard in shape as compared to monofilament.

From Table 2, it is evident that the PVA fibres are macrofibres, while PP fibres are microfibres. Thus, it is expected that PVA fibres may bear more loads and bridging cracks after concrete matrix breaks. On the other hand, the PP fibres may able to manage the initial cracking due to shrinkage.

The mix proportions and nomenclature are mentioned in Table 3. The mix proportion has been set based on trials and found suitable for self-compacting fibre-reinforced concrete.

2.1 Specimen Mixing, Casting, and Testing Details

The concrete was mixed in a drum mixer of 100-L capacity as per the European Guidelines' instruction (EFNARC) (BIBM, and EFNARC 2005), as shown in Fig. 2.

Fig. 1 Polypropylene (monofilament and fibrillated types) and polyvinyl alcohol fibres used

Table 2 Physical properties of PVA and PP fibres

*Fibre details	PVA fibres	Monofilament PP fibres	Fibrillated PP fibres
Fibre type	Straw type	monofilament	Fibrillated
Diameter (μm)	660	20	20
Cut length (mm)	30	13, 19,25	13, 19,25
Tensile strength (MPa)	900	407.2	407.2
Elastic modulus (GPa)	23	0.65	0.65
Specific gravity	1.3	0.91	0.91
Elongation (%)	7	25	25

*All properties given in this table are provided by the supplier

The rheological properties of 14 (SCC, SCC-FRC, and hybrid SCC-FRC) mixes were determined by performing slump-flow, V-funnel, and L-box tests as specified by the EFNARC standard (BIBM, and EFNARC 2005). Table 4 shows the characteristics, test method, and the typical value range of different SCC tests recommended by the EFNARC (BIBM, and EFNARC 2005) to qualify for different structural applications. Therefore, a varying amount of VMA was used in all 14 mixes for their qualification in the fresh state. The results of rheological property are presented and discussed in the forthcoming section.

The concrete slump flow of the mixes at different fibre volume fractions was tested as per EFNARC (BIBM, and EFNARC 2005). The flow spread was calculated using Eq. (1):

$$\boldsymbol{S} = \frac{\boldsymbol{d}_{\max} + \boldsymbol{d}_{\min}\boldsymbol{ord}_{\text{perp}}}{2}. \tag{1}$$

In Eq. (1), "S" represents the flow spread, "d_{max}" is the maximum spread diameter, and "d_{min}" is the diameter measured perpendicular to the d_{max}.

The L-box test results were expressed in terms of the passing ratio (PA) or the blocking ratio (BL) calculated by using Eq. (2) and Eq. (3). Only those mixes qualified as SCC, based on L-box tests, were used to cast specimens.

$$\boldsymbol{PA} = \frac{\boldsymbol{H}}{\boldsymbol{H}_{\max}} \tag{2}$$

$$\boldsymbol{BL} = 1 - \frac{\boldsymbol{H}}{\boldsymbol{H}_{\max}}. \tag{3}$$

In Eqs. (2) and (3), "PA" is the passing ratio, "BL" is the blocking ratio, "H" is the height of concrete at the edge of the horizontal side of the L-box, and "$H_{\max}$" is 91 mm. $H_{\max}$ is an ideal height when the vertical hopper contains exactly 12.7 L of SCC and completely levels in the test.

By the careful analysis of the mixes, the segregation can be determined through the J-ring test. Equations (4) and (5) were used to calculate the parameters given as:

$$Sj = \frac{d_{max} + d_{perp}}{2} \tag{4}$$

$$Bj = \frac{\Delta hx1 + \Delta hx2 + \Delta hy1 + \Delta hy2}{4} - \Delta h0 \tag{5}$$

where "$\boldsymbol{Sj}$" represents the flow spread, "$d_{\max}$" is the maximum spread diameter, and "d_{perp}" is the diameter perpendicular to the maximum spread. There were four positions outside the J-ring marked. Two were in the horizontal direction (*i.e.*$\Delta hx1$, $\Delta hx2$), and the other two were in the vertical direction (*i.e*, $\Delta hy1$, $\Delta hy2$).

Here,

"$\Delta hx1$" is the relative difference between J-ring height and concrete height near the base at the maximum spread on the one side.

"$\Delta hx2$" is the difference between J-ring height and concrete height near the base at the maximum spread on the other side.

"$\Delta hy1$" is the difference between J-ring height and concrete height near the base at the line perpendicular to the maximum spread on the one side.

Table 3 SCC, SCC-FRC, and hybrid SCC-FRC mixes proportions and their nomenclature

Mix ID	Concrete material ingredients (kg/m^3)					Fibre properties		Remarks
	Cement	Fly ash	Fine aggregates	Coarse aggregates	w/b ratio	PVA fibre %, (length, mm)	PP fibre %, (length, mm)	
M-0	420	180	900	750	0.35	0	0	SCC control mix without PVA and PP fibres
M-P	420	180	900	750	0.35	2 (30)	0	SCC-FRC mix having 2% of PVA fibres of 30 mm length
M-M13	420	180	900	750	0.35	0	2 (13)	SCC-FRC mix having 2% of "monofilament" PP fibres of 13 mm length
M-F13	420	180	900	750	0.35	0	2 (13)	SCC-FRC mix having 2% of "fibrillated" PP fibres of 13 mm length
M-M19	420	180	900	750	0.35	0	2 (19)	SCC-FRC mix having 2% of "monofilament" PP fibres of 19 mm length
M-F19	420	180	900	750	0.35	0	2 (19)	SCC-FRC mix having 2% of "fibrillated" PP fibres of 19 mm length
M-M25	420	180	900	750	0.35	0	2 (25)	SCC-FRC mix having 2% of "monofilament" PP fibres of 25 mm length
M-F25	420	180	900	750	0.35	0	2 (25)	SCC-FRC mix having 2% of "fibrillated" PP fibres of 25 mm length
M-PM13	420	180	900	750	0.35	1.5 (30)	0.5 (13)	Hybrid SCC-FRC mix having 1.5% and 0.5% s of PVA and PP "monofilament" fibres of 30 mm and 13 mm lengths
M-PF13	420	180	900	750	0.35	1.5 (30)	0.5 (13)	Hybrid SCC-FRC mix having 1.5% and 0.5% s of PVA and "fibrillated" PP fibres of 30 mm and 13 mm lengths
M-PM19	420	180	900	750	0.35	1.5 (30)	0.5 (19)	Hybrid SCC-FRC mix having 1.5% and 0.5% s of PVA and "monofilament" PP fibres of 30 mm and 19 mm lengths
M-PF19	420	180	900	750	0.35	1.5 (30)	0.5 (19)	Hybrid SCC-FRC mix having 1.5% and 0.5% s of PVA and "fibrillated" PP fibres of 30 mm and 19 mm lengths
M-PM25	420	180	900	750	0.35	1.5 (30)	0.5 (25)	Hybrid SCC-FRC mix having 1.5% and 0.5% s of PVA and "monofilament" PP fibres of 30 mm and 25 mm lengths
M-PF25	420	180	900	750	0.35	1.5 (30)	0.5 (25)	Hybrid SCC-FRC mix having 1.5% and 0.5% of PVA and "fibrillated" PP fibres of 30 mm and 25 mm lengths

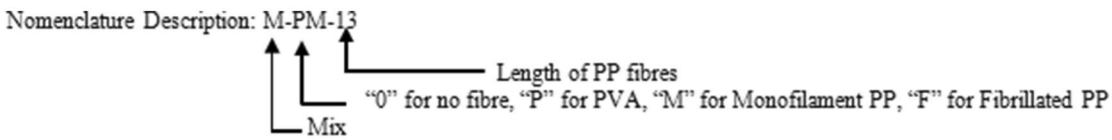

"Δ*hy*2" is the difference between J-ring height and concrete height near the base at the line perpendicular to the maximum spread on the one side.

"Δ*h*0" is the relative difference between the rod's edge and the concrete surface at the central position.

After obtaining adequate rheological properties, the required specimens for compression, split tension, direct tension, and flexural tests were cast. Table 5 describes the size and number of specimens with the standards used. Figure 3 shows the casting of specimens. After casting, the specimens were kept for 24 h in the laboratory environment for hardening and then soaked in a water tank for 28 days after unmoulding.

The cylindrical specimens were tested under compression in Universal Testing Machine (UTM) as per ASTM C39 (ASTM C39, C39M-12(2012), "Standard Test Method for Compressive Strength of Cylindrical Concrete Specimens", ASTM, 2012) with a deformation rate of 0.5 mm/min. Figure 4 shows the testing setup of the cylinders. The linear variable differential transducer (LVDT) on the gauge length of 100 mm was used to measure the deformation under load (Figs. 5, 6).

Fig. 2 Hybrid SCC-FRC mixing sequence

Table 4 Characteristics, test method(s), and corresponding ranges of values for SCC (BIBM, and EFNARC 2005)

Characteristic	Test method(s)	Unit	The typical range of values	
			Minimum	Maximum
Flowability	Slump flow (SF)	mm	650	800
Viscosity	T_{50} slump flow or V-funnel	Sec	2	5
Passing ability or a passing ratio (PA)	L-Box	–	0.75	1.0

Table 5 Testing and casting detail of the specimens

Test	Specimen size, mm	Number of specimens	Reference standard
Compression	100 dia × 200 height cylinder	3 specimens × 14 mixes = 42	ASTM C39 (ASTM C39, C39M-12(2012), "Standard Test Method for Compressive Strength of Cylindrical Concrete Specimens", ASTM, 2012)
Split Tension	100 dia × 200 height cylinder	3 specimens × 14 mixes = 42	ASTM C496 (ASTM C496, C496M-11(2011), "Standard Test Method for Splitting Tensile Strength of Cylindrical Concrete Specimens" 2011)
Flexure	100 × 100 × 500 prism	3 specimens × 14 mixes = 42	ASTM C78 (ASTM C78–10(2010), "Standard Test Method for Flexural Strength of Concrete (Using Simple Beam with Third-Point Loading)" 2010)
Direct tension	70 × 100 × 450 prism, a notch of 15 mm on both face at the middle	3 specimens × 14 mixes = 42	–

The split tensile test was performed using a compression testing machine (CTM) following the procedure specified in ASTM C496 (ASTM C496, C496M-11(2011), "Standard Test Method for Splitting Tensile Strength of Cylindrical Concrete Specimens" 2011) and is shown in Fig. 7. The loading rate was kept constant as equal to 5 mm/min. The test was performed on three cylindrical specimens (100 mm diameter × 200 mm height). The average result of the three values was used to calculate the splitting tensile strength using Eq. (6).

$$f'sp = \frac{2P}{\pi LD} \tag{6}$$

In Eq. (6), "f'_{sp}" represents the tensile splitting strength, "P" is the compressive load applied on the cylinder, "D"

Fig. 3 Specimen casting detail

Fig. 4 Cylinders tested to compression

is the diameter of the cylinder, and "*L*" is the length of the cylinder. The values thus obtained were compared with each other to determine the indication of any variation or trend.

The four-point bending test was conducted on the prisms having the sizes given in Table 4 following the (Fig. 8) procedure specified in ASTM standard C78 (ASTM C78-10(2010), "Standard Test Method for Flexural Strength of Concrete (Using Simple Beam with Third-Point Loading)" 2010). The flexure test performed using a Universal Testing Machine (UTM), and shown in Fig. 9, load–deflection behaviour and flexural strengths were determined. The load vs. deflection curves were plotted using a data logger.

There are no standards for the direct tension test of the concrete because of trouble in controlling different affecting parameters, for example, the size and shape of the sample (Yokota et al. 2008; Benson and Karihaloo 2005), sample gripping (Benson and Karihaloo 2005), gauge length (Benson and Karihaloo 2005), and the loading rate. In the literature, cylinder-, prism-, and dog-bone-shaped specimens with and without notch are used for the direct tension test of mortar or cementitious composites (Yokota et al. 2008; Benson and Karihaloo 2005). In the direct tension test, the specimen shape is a problem that may cause bond failure due to stress concentration at the interface of the specimen and steel loading plate. Therefore, a dog-bone-shaped specimen is a better choice to minimise the chances of bond failure (Benson and Karihaloo 2005) in cementitious composites. Practically, the casting of a dog-bone-shaped specimen (Figs. 10, 11, 12, 13) using concrete is not possible due to the larger size required to avoid the effect of the specimen size, as reported by Naaman and Reinhardt (Naaman and Reinhardt 2006). Therefore, a prism-shaped specimen with a notch in the middle half-length was used, as shown in Fig. 14. The specimen shape used in this study was similar to the one used by

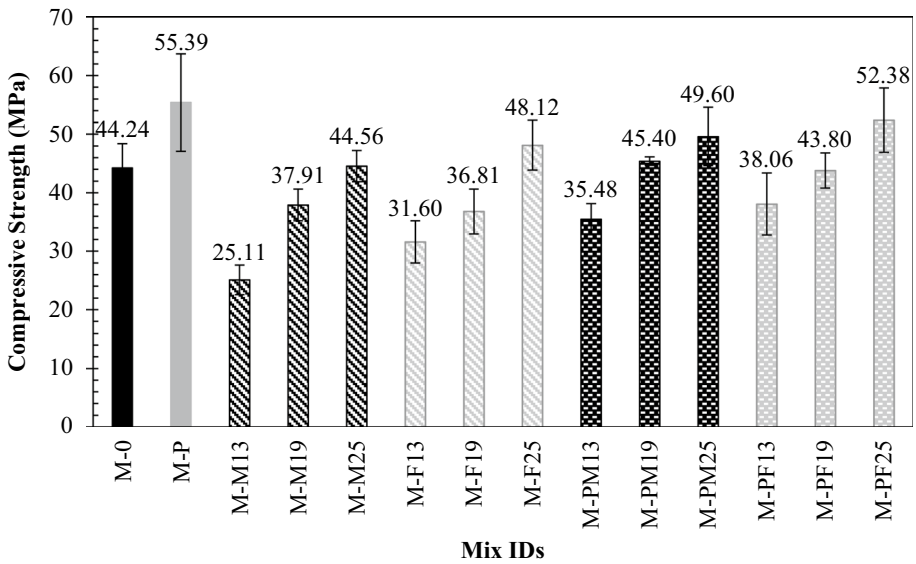

Fig. 5 Compressive strength of SCC, SCC-FRC, and hybrid SCC-FRC mixes

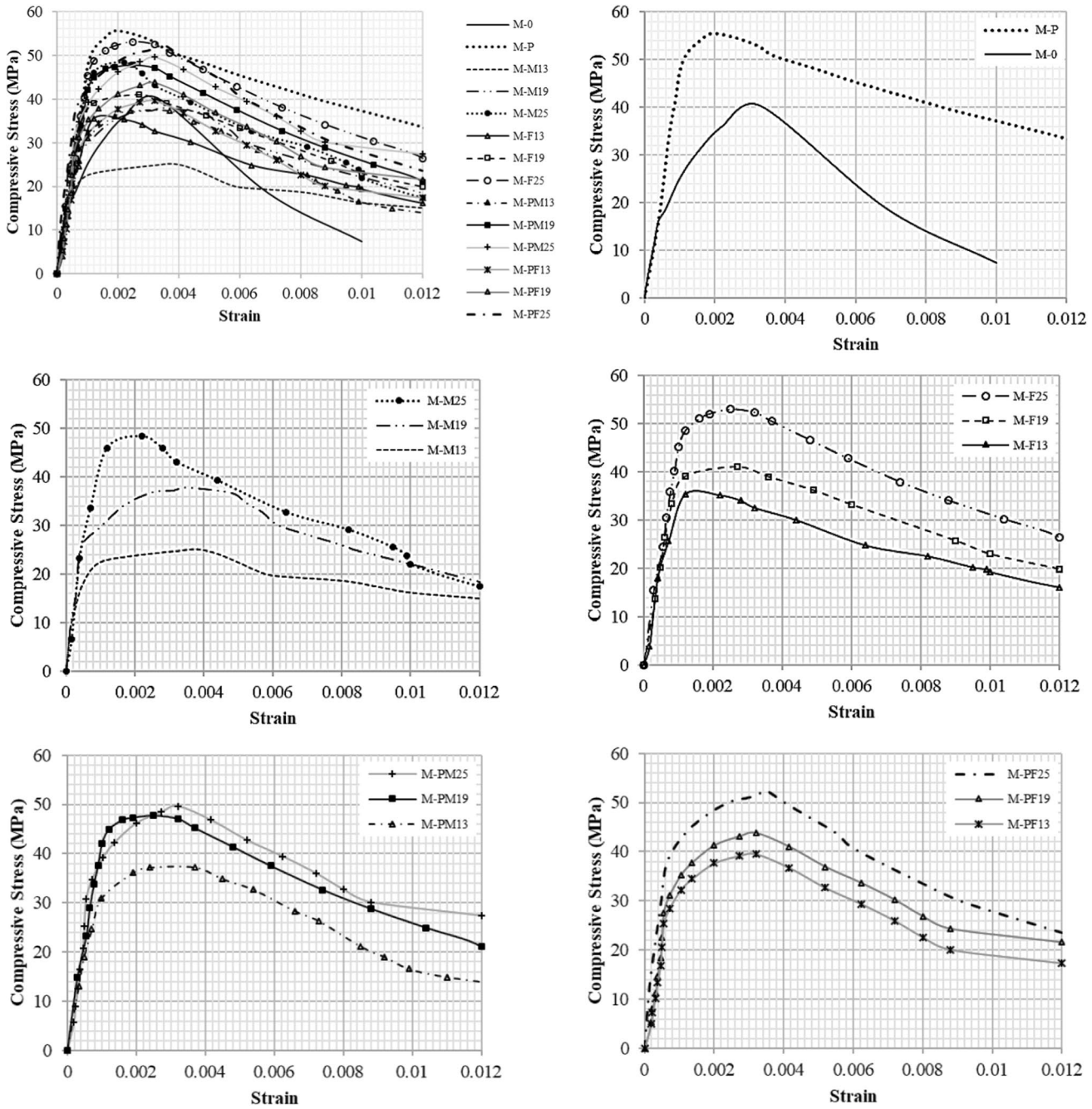

Fig. 6 Stress–strain response of all mixes under compression

Lim *et* al. (Lim et al. 1987) for SFRC. The steel deformed bars were embedded concentrically on the two sides of the concrete prism of 100 × 100 × 450 mm in size to evade the bond failure and misalignment of the specimen. The two deformed bars (each was 300 mm in length) were embedded up to 150 mm deep in the concrete aligned with the prism length, as shown in Fig. 14. A 15-mm-deep V-notch was provided in the middle half-length of the beam on the two faces to localise the failure plane, as shown in Fig. 14. The cross section of the prism specimen in the present study was 100 mm × 100 mm, which was reduced to 70 mm × 100 mm due to the notches. Benson and Karihaloo (2005) stated that the appearance of multiple cracking is not possible in the notched specimen subjected to direct tensile load due to the weakest point caused by the notch and the reduced cross section at the middle half-length. LVDT was used to measure the deformation over the gauge length of 150 mm, as shown in Fig. 14.

Fig. 7 Cylinder tested for a split tension

3 Experimental Results

3.1 Rheological Properties

3.1.1 Slump-Flow Test

The two slump-flow parameters, i.e. flow spread and the time required for the flow of concrete to spread up to a 500 mm diameter (T50), were measured. The flow spread indicates the free, unrestricted deformability, and the time indicates the rate of deformation for spread up to a 500 mm diameter (Neville 2010). Table 6 represents the results of the slump-flow test.

In all the mixes, the time required to flow up to a diameter of 500 mm (T50) was less than 5 s, and the slump-flow spread was more significant than 700 mm. The maximum spread was observed in the control mix without fibre (M-0). The minimum spread was observed in the mix with fibrillated PP fibres of length 25 mm (M-F25). The slump-flow test results shown in Table 6 may suggest that all mixes were exhibiting self-compacting behaviour.

3.1.2 L-Box Test

L-Box test measures fresh SCC's passing ability to pass through the specified gaps of steel bars and flowing within a defined flow distance once it drops from a certain height (BIBM, and EFNARC 2005). The results presented in Table 7 suggest that the passing ratio (PA) of the control mix was higher, and it was equal to 0.84. The minimum PA ratio was 0.68 for the mix M-F19 (the mix containing 19-mm-long fibrillated PP fibres). The blocking ratio of the SCC mix containing fibrillated PP fibres resulted in the greatest value; however, all mixes conform to the recommended value range of SCC.

Fig. 9 Flexure test set-up

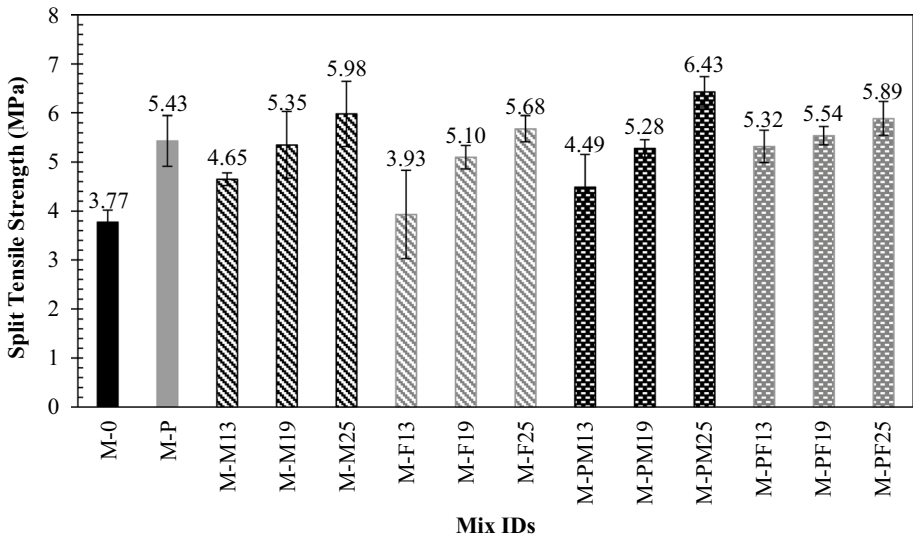

Fig. 8 Tensile splitting strength results of SCC, SCC-FRC, and hybrid SCC-FRC mixes

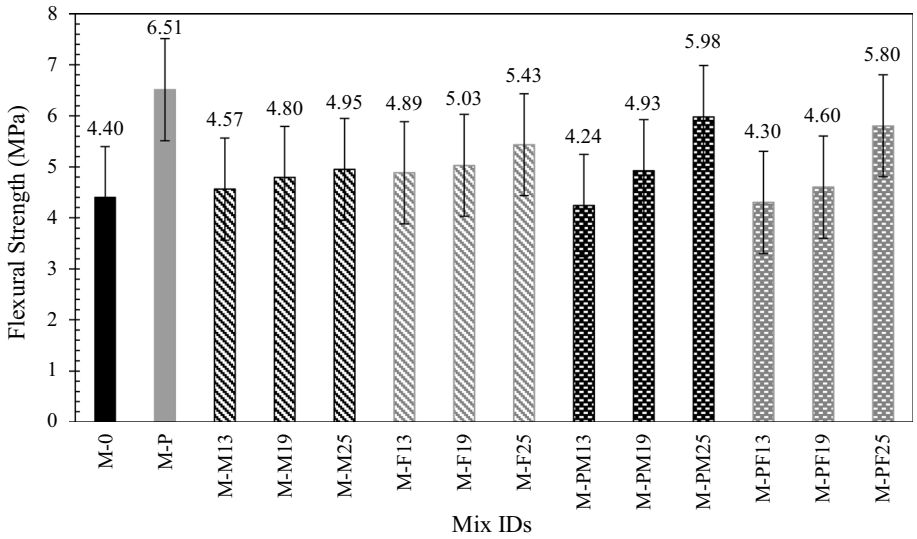

Fig. 10 Flexure test results of SCC, SCC-FRC, and hybrid SCC-FRC mixes

3.1.3 J-Ring Test

The J-ring test also confirmed the filling ability and passing ability of SCC, SCC-FRC, and hybrid SCC-FRC. The J-ring test measures the flow spread (*Sj*), flow time (*T*50*J*), and blocking step (*Bj*). The flow spread and the flow time give the filling ability, while the blocking step indicates the concrete's passing ability. Table 8 shows the J-ring test results. EFNARC (BIBM, and EFNARC 2005) does not recommend the J-ring test; however, this test is a good contender for finding the passing ability on site. Thus, the test procedure and specification were adopted, as suggested by De Schutter (De Schutter 2005).

The J-ring flow time T50J in all mixes was closed to 3.5 s, which is the optimum value. The flow spread of the control mix with no fibre was higher, whereas the blocking step Bj was within the specified limits in almost all the mixes except the mix with monofilament PP fibres of length 13 mm (M-M13).

3.2 Properties of Hardened Concrete

Once the confirmatory rheological properties were acquired, the specimens were cast and then cured for 28 days. The detail of the specimens is given in Table 5. After completing the curing period, the cylinders were capped with the sulphur as per ASTM C 469 (ASTM C469(2001), "Standard Test Method for Static Modulus of Elasticity and Poisson's Ratio of Concrete in Compression", ASTM, 2001). The detail of the tests performed and their results are given in the following.

3.2.1 Compression Test

Figures 5 and 6 show the compressive strengths and the compressive stress–strain responses of all SCC mixes. The SCC mix containing PVA fibres (i.e. mix M-P) had maximum compressive strength, 55.39 MPa. Simultaneously, the compressive strength of the control SCC mix (i.e. mix M-0) was 44.24 MPa, which shows that the addition of PVA fibres increased strength by 25% than the control SCC mix without fibres.

The compressive strength of SCC mixes containing monofilament PP fibres (mixes M-M13, M-M19, and M-M25) and fibrillated PP fibres (mixes M-F13, M-F19, and M-F25) showed lesser results as compared to the SCC mix containing PVA fibres (mix M-P). The reduction in compressive strength in the mixes M-M13, M-M19, and M-M25 was 54.67, 31.56, and 19.55%, respectively, compared to the mix M-P, whereas the compressive strength of mixes M-F13, M-F19, and M-F25 was reduced by 42.95, 33.54, and 13.13%, respectively, than the mix M-P. The overall compressive strength of the SCC mix with fibrillated fibres was higher than the SCC mixes with monofilament fibres.

The percentage reduction compared with the control mix M-0 (without fibres) was significantly higher than the mix M-P (containing 2% PVA fibre volume). The reduction in compressive strength in the mixes M-M13, M-M19, and M-M25 was 54.67, 31.56, and 19.55%, respectively, compared to mix M-P, whereas the compressive strength of mixes M-F13, M-F19, and M-F25 was reduced by 42.95, 33.54, and 13.13%, respectively, compared to mix M-P. The increase in the compressive strengths was found in mixes having longer monofilament PP fibres. A similar trend was

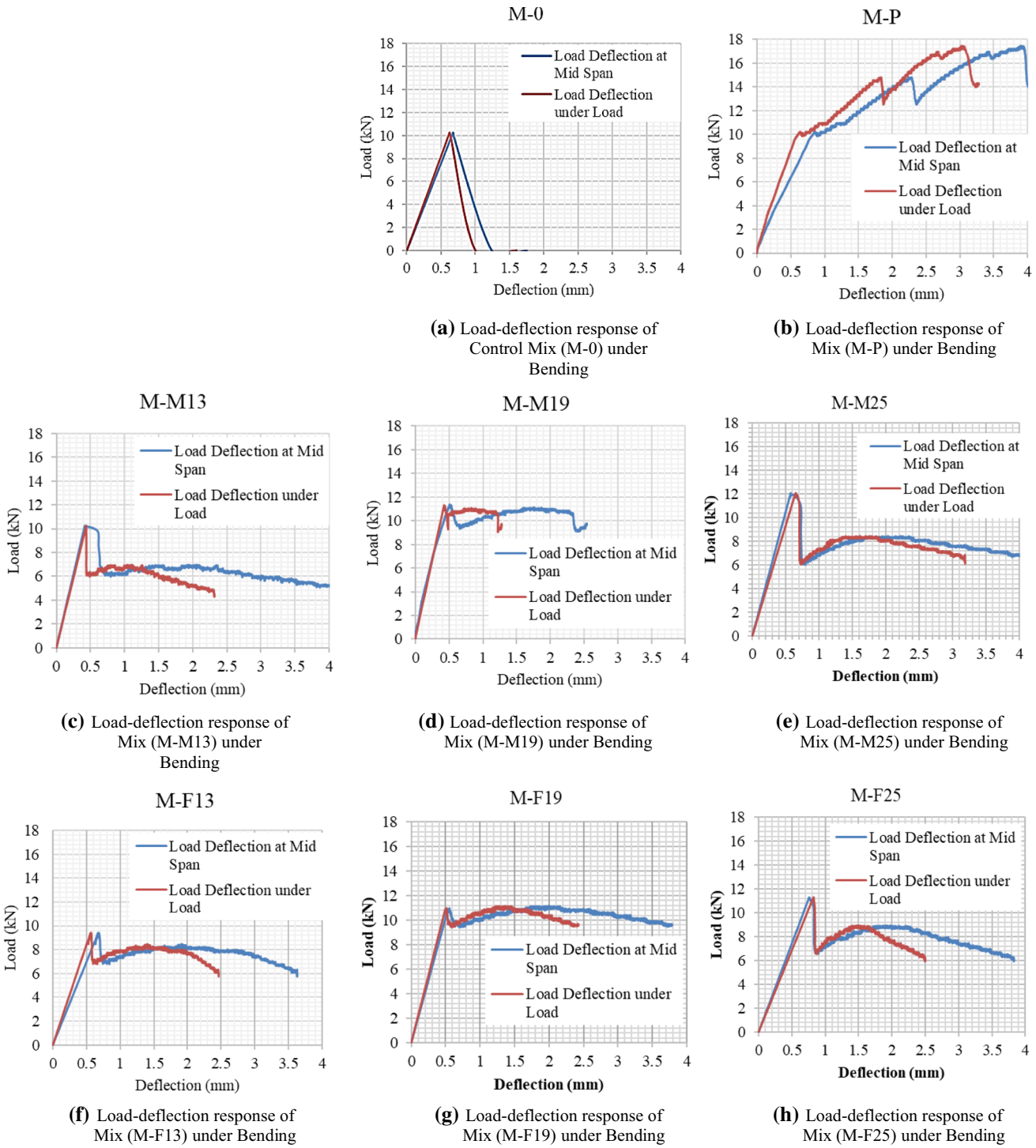

(a) Load-deflection response of Control Mix (M-0) under Bending

(b) Load-deflection response of Mix (M-P) under Bending

(c) Load-deflection response of Mix (M-M13) under Bending

(d) Load-deflection response of Mix (M-M19) under Bending

(e) Load-deflection response of Mix (M-M25) under Bending

(f) Load-deflection response of Mix (M-F13) under Bending

(g) Load-deflection response of Mix (M-F19) under Bending

(h) Load-deflection response of Mix (M-F25) under Bending

Fig. 11 Load–deflection response of SCC and SCC-FRC mixes under flexure

also observed in the SCC mixes having long fibrillated PP fibres (mix M-F25). Overall, the compressive strength of SCC mixes containing fibrillated fibres was higher.

The compressive strength and the stress–strain response of hybrid SCC-FRC mixes (containing a hybrid of PVA fibres with monofilament and fibrillated fibres) were the best. They improved as compared to the SCC mixes containing PP fibres. The trend of increase in the compressive strength of hybrid SCC-FRC mixes was similar to the SCC-FRC mixes containing either monofilament or fibrillated PP fibres.

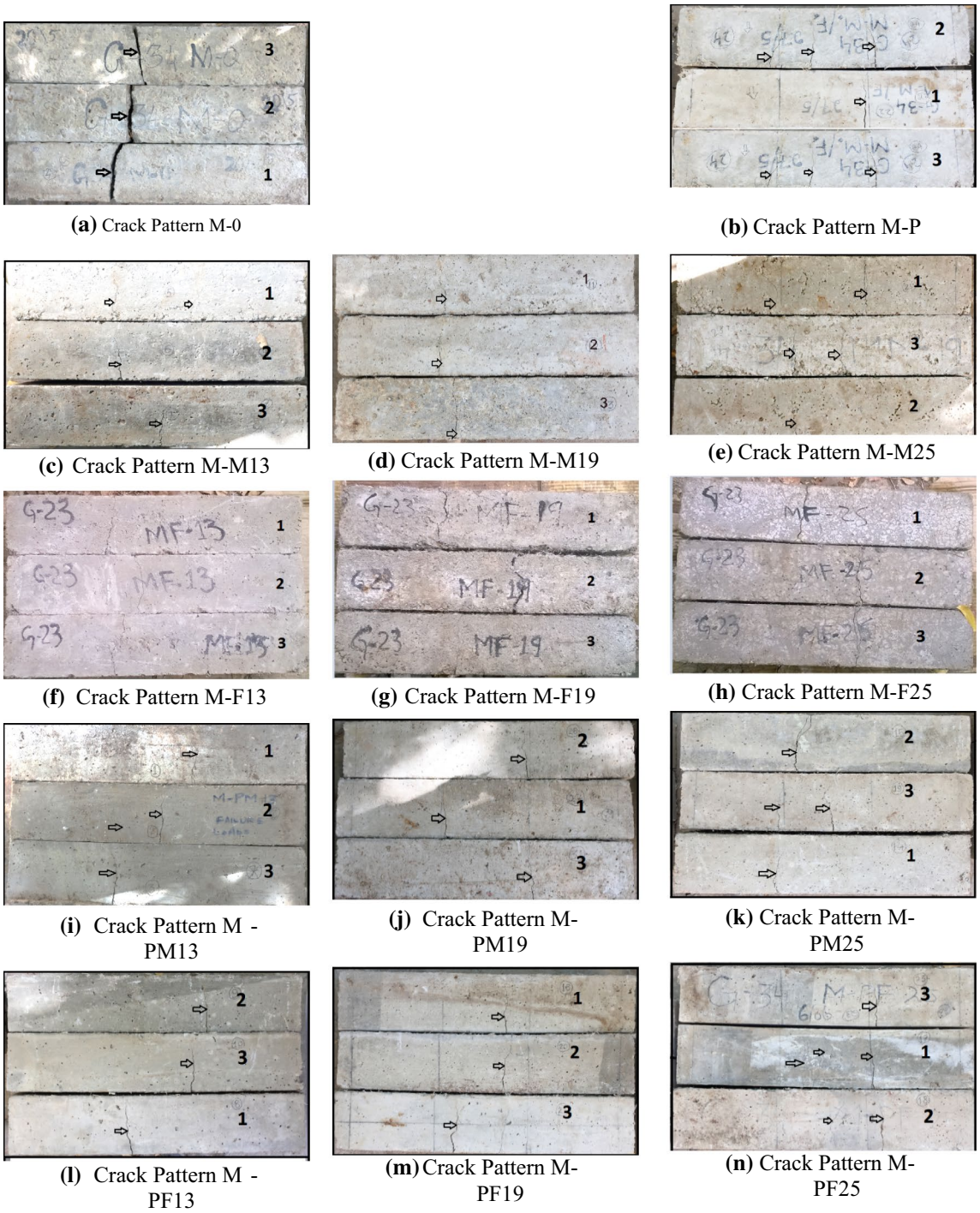

(a) Crack Pattern M-0

(b) Crack Pattern M-P

(c) Crack Pattern M-M13

(d) Crack Pattern M-M19

(e) Crack Pattern M-M25

(f) Crack Pattern M-F13

(g) Crack Pattern M-F19

(h) Crack Pattern M-F25

(i) Crack Pattern M - PM13

(j) Crack Pattern M-PM19

(k) Crack Pattern M-PM25

(l) Crack Pattern M - PF13

(m) Crack Pattern M-PF19

(n) Crack Pattern M-PF25

Fig. 12 Crack patterns of beams after testing under flexure

It infers that the hybridisation of PVA fibres with monofilament and fibrillated PP fibres is promising for the structural application. In general, the PVA hybrid with fibrillated PP fibres gave a better response than the PVA hybrid with monofilament PP fibres.

Figure 6 shows the compressive stress–strain responses of SCC mixes with and without fibres. This behaviour may explain by comparing the pre-peak stress responses in the pre- and post-peak branches of the stress–strain curves. The slope in the ascending branch is identical in all stress–strain curves irrespective of the type of fibres. This response suggests that concrete response in terms of elastic modulus primarily depends on the matrix rather than fibres, which is also reported by several pieces of research on FRC (Ayub

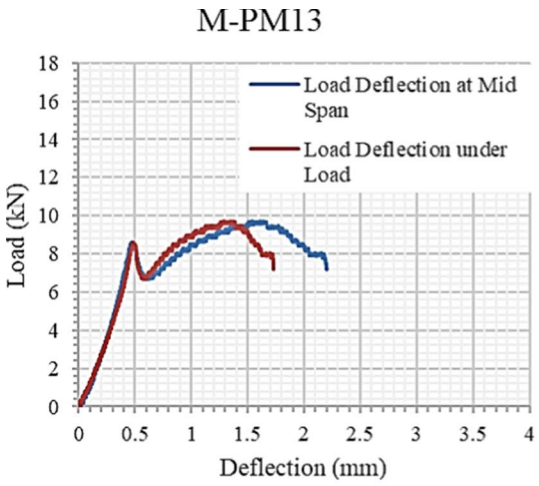

(a) Load-deflection response of Mix (M-PM13) under Bending

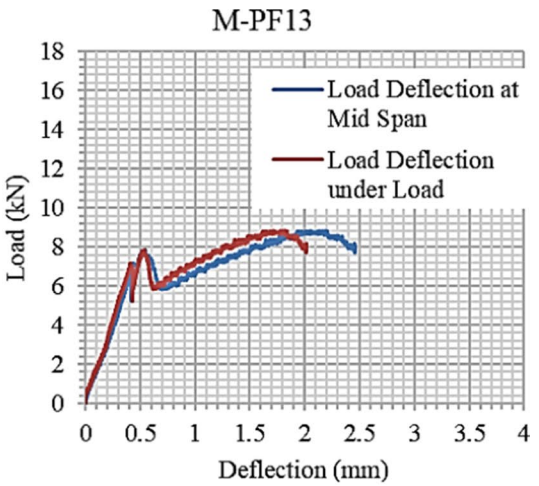

(d) Load-deflection response of Mix (M-PF13) under Bending

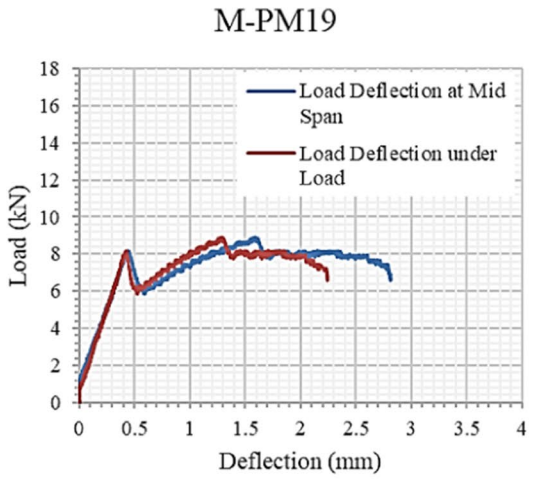

(b) Load-deflection response of Mix (M-PM19) under Bending

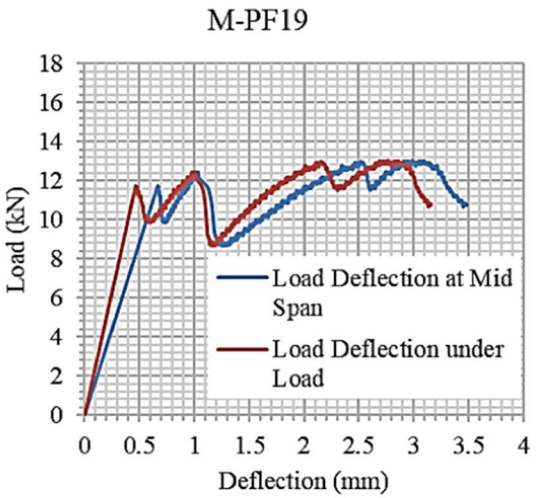

(e) Load-deflection response of Mix (M-PF19) under Bending

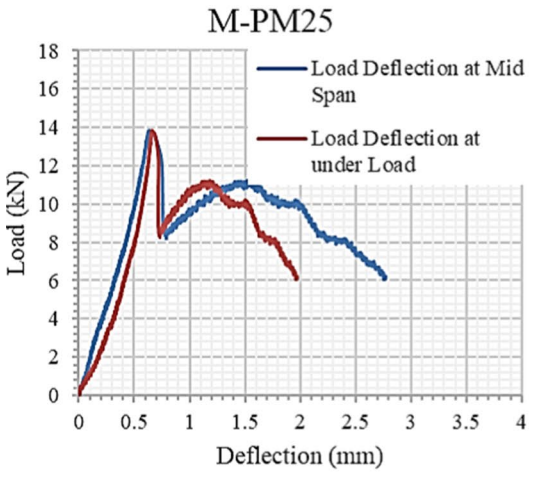

(c) Load-deflection response of Mix (M-PM25) under Bending

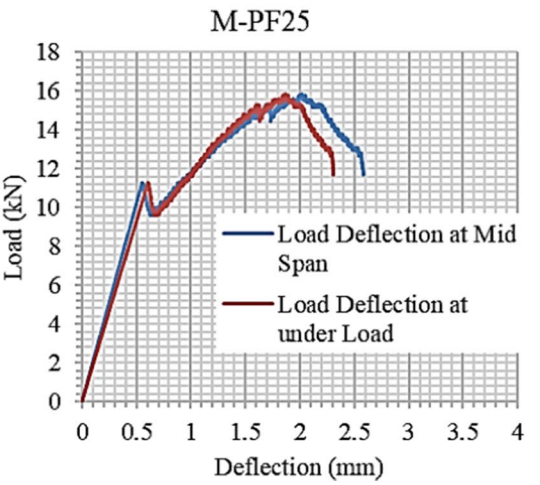

(f) Load-deflection response of Mix (M-PF25) under Bending

Fig. 13 Load–deflection response of SCC, SCC-FRC, and hybrid SCC-FRC mixes under bending

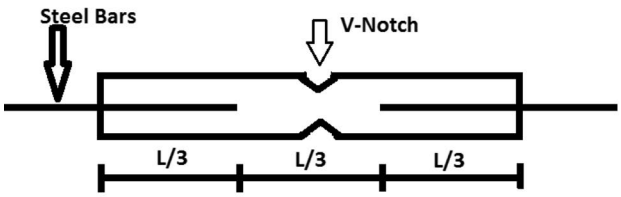

(Direct tension test specimen)

Fig. 14 Direct tension test set-up

Table 6 Slump-flow results of SCC, SCC-FRC, and hybrid SCC-FRC mixes

Mix IDs	T50 (sec)	dmax (mm)	dperp (mm)	$S = \frac{d_{max}+d_{perp}}{2}$ (mm)	Minimum limit as per (BIBM, and EFNARC 2005)	Maximum limit as per (BIBM, and EFNARC 2005)	Remarks
M-0	3.53	870	850	860	The minimum limit of slump flow is 650 mm	The maximum limit of slump flow is 800 mm	All mixes are qualifying the minimum slump-flow requirement
M-P	3.67	850	840	845			
M-M13	4.88	790	790	790			
M-M19	4.84	770	760	765			
M-M25	4.89	750	760	755			
M-PM13	3.99	820	790	805			
M-PM19	3.98	810	780	795			
M-PM25	3.87	790	810	800	Minimum flow time T50 is 2 s	Maximum flow time T50 is 5 s	
M-F13	4.78	770	750	760			
M-F19	4.67	780	760	770			
M-F25	4.89	750	750	750			
M-PF13	3.44	810	820	815			
M-PF19	3.92	830	790	810			
M-PF25	3.67	800	810	805			

et al. 2015; 544.1R-96 2002). The strength was substantially increased with PVA fibres alone and with fibrillated PP fibres of the length of 25 mm as a hybrid. The reason might be the confinement provided by the fibres in the cylindrical specimens by holding the shape on the higher load. The strain at the peak stress is varying from 0.002 to 0.0035.

In the descending branch of stress–strain curves of SCC, the steepness in the curve was less with the fibres having a higher aspect ratio (or long length), which is also reported in ACI 544.1R-96 (544.1R-96 2002). The concrete with PVA fibres (mix M-P) exhibited the most improved response due to the long length of PVA fibres (30 mm). The hybrid SCC-FRC response containing PP and PVA fibres was also improved, as shown in Fig. 6. The maximum size of aggregate used in all mixes was 12 mm, and the mixes containing fibres having a length more than the size of the aggregates showed a better bridging and improvement in the descending branch. The improved response might be the concrete containing 19 mm or higher a length of PP fibres, which improved the response in the falling branch. Jenq and Shah (1986) also reported a similar reason that the response of FRC to sustain loads is higher if there was more length of fibres embedded in the cement matrix.

Table 7 Results of the L-box test

Mix IDs	Δh (mm)	H = 150—Δh (mm)	Hmax (mm)	$PA = \frac{H}{Hmax}$	$BL = 1 - \frac{H}{Hmax}$	Recommended value of the passing ratio (PA) and blocking ratio (BL) (BIBM and EFNARC 2005)	Remarks
M-0	67	83	91	0.91	0.09	$0.75 \le PA \le 1.0$ $0 \le BL \le 0.25$	The passing ratios (PA) and blocking ratios (BL) suggest the good passing ability of all mixes
M-P	71	79	91	0.87	0.13		
M-M13	78	72	91	0.79	0.21		
M-M19	78	72	91	0.79	0.21		
M-M25	69	81	91	0.89	0.11		
M-PM13	71	79	91	0.87	0.13		
M-PM19	73	77	91	0.85	0.15		
M-PM25	70	80	91	0.88	0.12		
M-F13	81	69	91	0.76	0.24		
M-F19	83	67	91	0.74	0.26		
M-F25	82	68	91	0.75	0.25		
M-PF13	76	74	91	0.81	0.19		
M-PF19	75	75	91	0.82	0.18		
M-PF25	74	76	91	0.84	0.16		

Table 8 J-Ring test results

Mix IDs	$T50J$(sec)	$dmax$(mm)	$dperp$ (mm)	Δho (mm)	$\Delta hx1$ (mm)	$\Delta hx2$ (mm)	$\Delta hy1$ (mm)	$\Delta hy2$ (mm)	Bj (mm)	Sj (mm)	Recommended values (Song et al2005) (mm)
M-0	3.1	708	690	102	118	117	120	114	15.25	699	$600 \le Sj \le 700$ $T50J \le 3.5$ $Bj \le 20$
M-P	3.6	610	605	108	129	123	127	123	17.5	607.5	
M-M13	4.2	597	588	111	135	132	135	129	21.75	592.5	
M-M19	4.4	591	571	112	133	131	134	131	20.25	581	
M-M25	4.7	590	583	112	134	129	129	123	16.75	586.5	
M-PM13	3.7	599	598	107	130	127	127	125	19.75	598.5	
M-PM19	3.6	596	590	109	131	123	123	121	17	593	
M-PM25	3.8	599	591	111	138	125	125	124	19.25	595	
M-F13	4.2	587	587	109	127	124	124	123	15.5	587	
M-F19	4.3	578	578	111	125	123	123	123	11.5	578	
M-F25	4.8	583	582	108	134	123	123	114	17.75	582.5	
M-PF13	3.9	584	582	109	125	138	138	118	16.75	583	
M-PF19	4.2	592	582	107	131	125	125	120	19.75	587	
M-PF25	3.7	589	553	104	116	124	124	123	16.5	571	

3.2.2 Split Tension Test

The result of the splitting tensile strength is presented in a bar chart, as shown in Fig. 8. The mix M-PM19 (containing 1.5 and 0.5% volume of PVA and monofilament PP fibres) shows the maximum tensile strength equal to 6.43 MPa. Overall, the mixes containing monofilament PP fibres resulted in maximum strength. The tensile splitting strength increased with the increase in the length of PP fibres. The reason for having higher splitting tensile strength might be the orientation of the monofilament during the casting of the cylinder. As fibrillated and PVA fibres tended to align vertically, there might be the least number of fibres aligned in the lateral direction in which split tensile force was applied.

3.2.3 Flexure Test

The flexural strength of each mix was determined and compared with the help of a bar chart, as shown in Fig. 10.

Figure 10 shows that the control mix resulted in the lowest flexural strength, which was 4.24 MPa, whereas the maximum strength of 6.51 MPa was observed in the SCC mix containing a 2% volume fraction of PVA fibres (mix M-P). The third maximum strength of 5.98 MPa was recorded in the mix M-PM25 (containing 1.5% and 0.5% volume fraction of PVA and monofilament PP fibres). Overall, the flexure strength and flexural response of the hybrid SCC-FRC were better than the other mixes.

Figures 11 and 12 represent the load–deflection response of all mixes. The control mix containing no fibres (mix M-0) failed without indicating any significant sign of failure or sustaining further load after cracking (refer to Fig. 11a). The prism made of mix M-0 (control mi concrete without fibres) showed a single crack, which was propagated towards the compression zone of the prism, as shown in Fig. 12a. This phenomenon was expected, as concrete cannot take tension without reinforcement or fibres. On the other hand, the mix M-P (containing a 2% volume fraction of PVA fibres) showed an increase in load even after the specimen cracking. The load–deflection response of mix M-P was similar to the Type III deflection-hardening response, as mentioned in ACI 544.1R-96 (544.1R-96 2002; Jenq and Shah 1986; Khan and Ayub 2016). The deflection-hardening response is well associated with PVA fibres and reported in several research pieces (Nuruddin et al. 2014; Khan and Ayub 2016; Holschemacher and Höer 2008b; Wang and Li 2003). This response is due to the bridging effect of PVA fibres, which increased the load with multiple cracking, as shown in Fig. 12b. The use of PP fibres in SCC mixes exhibited a Type II deflection-hardening response, as mentioned in ACI 544.1R-96 (Khan and Ayub 2016, 3R-93(1993), "ACI Committee 544.3r-93. Guide for Specifying, Proportioning, Mixing, Placing and Finishing Steel Fiber Reinforced Concrete" 1993), and shown in Fig. 11c–h. A drop in the load was observed after the development of the first crack. A single crack propagated into the compression zone of the prism specimens reinforced with PP fibres (refer to Fig. 12(c–h)). The response of SCC containing PP fibres can be explained based on the elastic modulus of fibres, as discussed in "Introduction" of this paper. PP fibre is a soft intruded fibre (Parameswaran 1991); therefore, a substantial increase in the load capacity was not expected; however, an increase in the deformation and strain capacity was expected, which is evident in Fig. 11(c–h).

The effect of the hybridisation of PVA and PP fibres in the load–deflection response of hybrid SCC-FRC prism specimens is shown in Fig. 13a–f, which is a Type III deflection-hardening response, as mentioned in ACI 544.1R-96 (3R-93(1993), "ACI Committee 544.3r-93. Guide for Specifying, Proportioning, Mixing, Placing and Finishing Steel Fiber Reinforced Concrete" 1993). The load was observed to be increasing even after the appearance of the cracks. The multiple cracking was also visualised on the specimens, as shown in Fig. 12(i–n).

Based on the flexural load–deflection responses of hybrid SCC-FRC mixes, it may infer that the hybridisation of PVA and PP fibres resulted in Type III deflection–hardening response, as mentioned in ACI 544.1R-96 (3R-93(1993), "ACI Committee 544.3r-93. Guide for Specifying, Proportioning, Mixing, Placing and Finishing Steel Fiber Reinforced Concrete" 1993). In terms of cost, the hybridisation of PVA and PP fibres is preferable as the PP fibres are 50% less expensive than PVA fibres. In the hybrid SCC-FRC mixes investigated in this study, PVA and PP fibres were used as 1.5% and 0.5% volume fraction of the total volume of concrete; however, there is an opportunity to investigate other fibre volume proportions. Therefore, it may recommend investigating other volume proportions of PVA and PP fibres in future studies. In the present study, hybrid SCC-FRC mixes qualified for the optimum response under flexure; therefore, it is necessary to investigate the direct tension response discussed in the forthcoming section.

3.2.4 Direct Tension Test

Figure 15 shows the results of the direct tension test in terms of tensile strength. The mix M-P (containing a 2% volume fraction of PVA fibres) resulted in the maximum tensile strength of 4.71 MPa. The results indicated the dependency of direct tensile strength on the fibre aspect ratio (or length of fibres); therefore, there was an increasing trend in the tensile strength with an increase in the aspect ratio (or fibre length). This trend may be the better bond between fibres and matrix, arresting micro-cracks due to the bridging effect, and improved tensile strength. The direct tension test results presented in Fig. 15 are against the results obtained under the split tension test shown in Fig. 8. The orientation of fibres in the case of the split tension test may affect the results.

On the other hand, the direct tension test performed using a prism specimen was having a random fibres orientation. The use of SCC also enhances the dispersion and random orientation of fibres. The direct tensile strength and response of SCHRC mix containing PVA and PP fibres of length 25 mm were higher and significantly improved and are coherent with the flexural test results.

Figure 16 represents the direct tensile load–deformation response. The mix M-P (containing a 2% volume fraction of PVA fibres) was significantly improved together with a remarkable strain-hardening response and a more than 1% strain capacity. The mix M-P after the cracking carried almost half of the peak load. The authors report a similar response in another study (Khan and Ayub 2016). This response is due to the slip-hardening behaviour of PVA fibres (Khan and Ayub 2016), which enabled the SCC mix

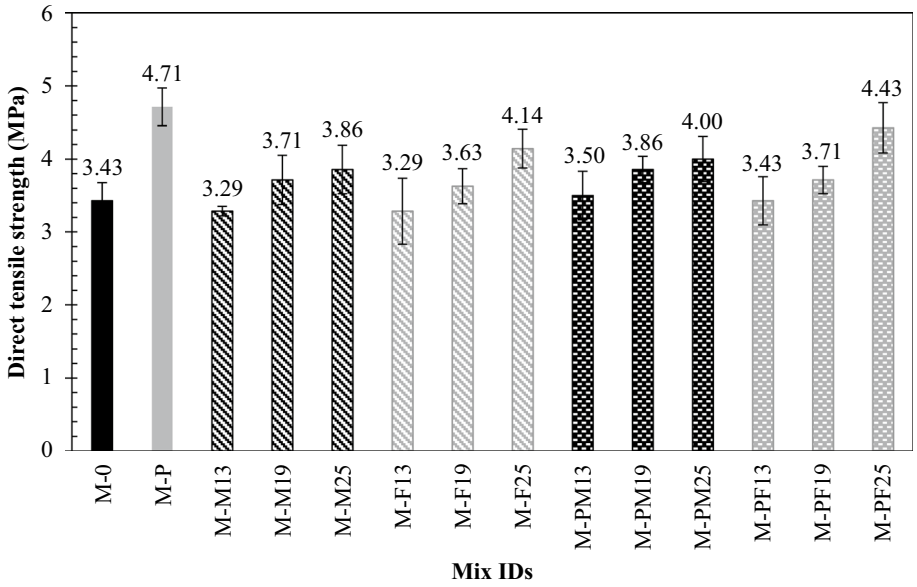

Fig. 15 Direct tension test results of SCC, SCC-FRC, and hybrid SCC-FRC

M-P to attain a higher strain capacity. The SCC mix containing PP fibres exhibited a small strain-hardening response after cracking with a substantial drop in the load, which may be due to the weak bond between PP fibres and the cement matrix (Zheng and Feldman 1995). The addition of PVA and PP fibres in hybrid SCC-FRC mixes exhibited a better response showing that both fibres complement each other and carried a significantly higher load after cracking, followed by the strain-hardening response due to the crack bridging. As a weak region intentionally created in the specimen in the form of the notch, that is why there was no multiple cracking observed in any specimen, which was as expected. Based on the result obtained by the direct tension test, it is implacably unfavourable the stand-alone use of PP fibres for structural purposes and higher mechanical properties; however, the hybrid use of PP fibres with PVA has apparent advantages. These benefits are higher mechanical properties and lower the cost of fibres compared to steel fibres. The strength-to-weight ratio of synthetic fibres causes lesser weight in an equivalent volume of steel fibres.

4 Conclusions and Recommendations

The following conclusions are drawn from the study:

1. The hybridisation of PVA and PP fibres in the SCC mixes advantageous in terms of higher mechanical properties and improved tensile strain capacity attainment.
2. J-ring test is an excellent test to assess the filling ability and passing ability; however, the test is adequate for the laboratory and only slump-flow and L-box tests are adequate for on-site construction.
3. The compressive, flexural, and tensile strengths increase with the increasing aspect ratio (or length) of PP fibres.
4. The hybrid of PVA and fibrillated PP fibres was better than a hybrid of PVA and monofilament PP fibres. This response is due to random orientation and better dispersion of fibrillated PP in the concrete.
5. The hybrid of PVA with monofilament PP and fibrillated PP fibres of 25 mm length showed a better post-peak response than the other fibre lengths. Thus, it may infer that the post-peak response under compression is dependent on the length of fibres.
6. Based on the response of hybrid SCC-FRC under flexure, it may infer that the hybridisation of PVA and PP fibres results in Type III deflection-hardening response. Thus, hybridisation is more beneficial and economical because 50% less cost of PP fibres is 50% than PVA fibres.
7. The use of SCC itself enhances the dispersion and random orientation of fibres. The results of direct tension tests are coherent with the flexural test results, and mixed use of PVA and PP fibres of length 25 mm has improved response.
8. The combination of PP with PVA fibres enhanced the strain capacity and strain-hardening response of hybrid SCC-FRC under direct tension.

Based on the conclusions, the use of PP fibres with PVA fibres is recommended. Further study is needed to explore the different proportions of PVA and PP fibres with varying binders and water contents to optimise hybrid PVA and PP fibres in SCC-FRC.

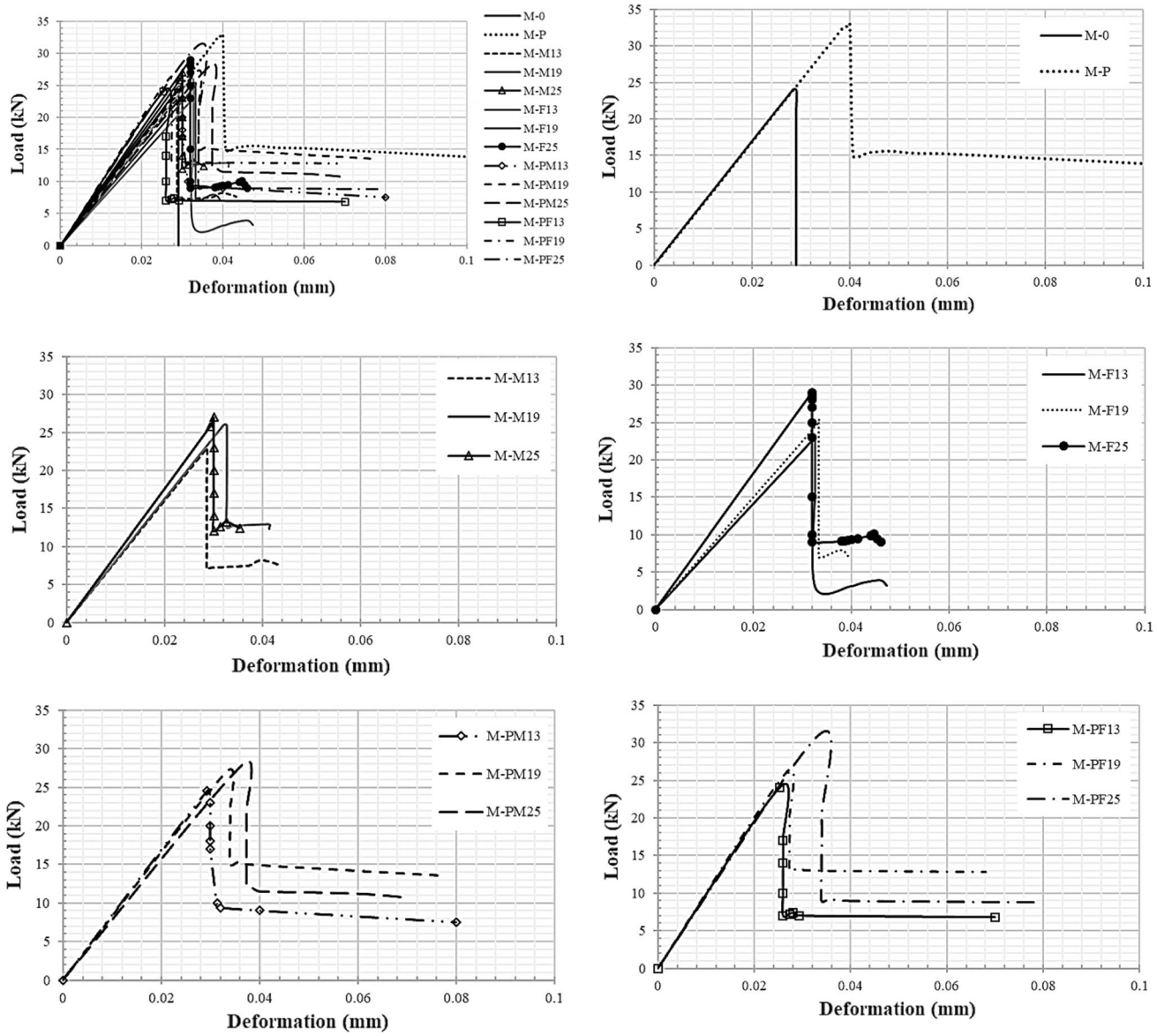

Fig. 16 Response of SCC, SCC-FRC, and hybrid SCC-FRC mixes under direct tension

References

544.1R-96 (2002) State of the Art Report on Fiber Reinforced Concrete Reported (Aci 544.1 R-96 Reapproved 2002)

"ACI Committee 544.3r-93. Guide for Specifying, Proportioning, Mixing, Placing and Finishing Steel Fiber Reinforced Concrete",

ASTM C 618 (2000), "Standard Specification for Coal Fly Ash and Raw or Calcined Natural Pozzolan for Use as a Mineral Admixture in Concrete", ASTM International

Abdul-Rahman, M, Al-Attar, AA, Hamada, HM, and Tayeh, B (2020), "Microstructure and Structural Analysis of Polypropylene Fibre Reinforced Reactive Powder Concrete Beams Exposed to Elevated Temperature", Journal of Building Engineering, 29, 101167

Afroughsabet V, Ozbakkaloglu T (2015) Mechanical and durability properties of high-strength concrete containing steel and polypropylene fibers. Constr Build Mater 94:73–82

Alani AM, Beckett D (2013) Mechanical properties of a large scale synthetic fibre reinforced concrete ground slab. Constr Build Mater 41:335–344

Al-Attar AA, Abdulrahman MB, Hamada HM, Tayeh BA (2020) Investigating the behaviour of hybrid fibre-reinforced reactive powder concrete beams after exposure to elevated temperatures. J Mater Res Technol 9:1966–1977

Asok, G, and George, S (2016), "Investigation on hybrid concrete using steel and polypropylene fiber", Int J New Technol Res, 2(5)

ASTM C 469 (2001), "Standard test method for static modulus of elasticity and Poisson's ratio of concrete in compression.", ASTM

ASTM C39/C39M-12 (2012), "Standard test method for compressive strength of cylindrical concrete specimens", ASTM

ASTM C496/C496M-11 (2011), "Standard test method for splitting tensile strength of cylindrical concrete specimens",

ASTM C78–10 (2010), "Standard test method for flexural strength of concrete (using simple beam with third-point loading)",

Ayub T, Shafiq N, Khan SU (2015) Compressive stress-strain behavior of HSFRC reinforced with basalt fibers. J Mater Civ Eng 28(4):06015014

Balouch S, Forth J, Granju J-L (2010) Surface corrosion of steel fibre reinforced concrete. Cem Concr Res 40(3):410–414

Benson SDP, Karihaloo BL (2005) Cardifrc®-development and mechanical properties. Part III: uniaxial tensile response and other mechanical properties. Mag Concr Res 57(8):433

BIBM, and EFNARC (2005), "The European guidelines for self-compacting concrete"

Chen Y, Qiao P (2011) Crack growth resistance of hybrid fiber-reinforced cement matrix composites. J Aerosp Eng 24(2):154–161

Corinaldesi V, Moriconi G (2012) Mechanical and thermal evaluation of ultra high performance fiber reinforced concretes for engineering applications. Constr Build Mater 26(1):289

de Azevedo AR, Marvila MT, Tayeh BA, Cecchin D, Pereira AC, Monteiro SN (2021) Technological performance of açaí natural fibre reinforced cement-based mortars. J Building Eng 33:101675

De Schutter, G (2005), "Guidelines for testing fresh self-compacting concrete", European research project

Empelmann M, Teutsch M, Steven, G (2008), "Improvement of the post fracture behaviour of UHPC by Fibres", Editor "Book Improvement of the Post Fracture Behaviour of UHPC by Fibres", Kassel University Press GmbH, 177

Etli S, Cemalgil S, Onat O (2018) Properties of self-compacting mortars with different contents of synthetic macro fiber. Academic Perspective Procedia 1(1):593–602

Granju J-L, Balouch SU (2005) Corrosion of steel fibre reinforced concrete from the cracks. Cem Concr Res 35(3):572

Haido JH, Abdul-Razzak AA, Al-Tayeb MM, Bakar BA, Yousif ST, Tayeh BA (2021) Dynamic response of reinforced concrete members incorporating steel fibers with different aspect ratios. Adv Concrete Const 11(2):89

Holschemacher K, Höer S (2008), "Influence of PVA fibers on load carrying capacity of concrete with coarse aggregates". BEFIB 2008: 7th RILEM International Symposium on Fibre Reinforced Concrete 219–2292008

Holschemacher K, Höer S (2008), "Influence of PVA Fibers on load carrying capacity of concrete with coarse aggregates", Editor "Book Influence of PVA Fibers on Load Carrying Capacity of Concrete with Coarse Aggregates", Chennai, India, 219

Hsie M, Tu C, Song P (2008) Mechanical properties of polypropylene hybrid fiber-reinforced concrete. Mater Sci Eng, A 494(1–2):153–157

Jenq Y, Shah SP (1986) Crack propagation in fiber-reinforced concrete. J Struct Eng 112(1):19–34

Kaufmann J, Frech K, Schuetz P, Münch B (2013) Rebound and orientation of fibers in wet sprayed concrete applications. Constr Build Mater 49:15–22

Khan SU, Ayub T (2016) Modelling of the pre and post-cracking response of the PVA fibre reinforced concrete subjected to direct tension. Constr Build Mater 120:540–557

Khan M, Cao M, Ali M (2020), "Cracking behaviour and constitutive modelling of hybrid fibre reinforced concrete", J Building Eng 30: 101272

Kim DJ, Park SH, Ryu GS, Koh KT (2011) Comparative flexural behavior of hybrid ultra high performance fiber reinforced concrete with different macro fibers. Constr Build Mater 25(11):4144–4155

KM, Af, and Varghese, S, (2014) Behavioral study of steel fiber and polypropylene fiber reinforced concrete. Int J Res Eng Technol 2(10):17–24

Li, VC (2008), "Engineered cementitious composites (ECC) material, structural, and durability performance"

Li B, Chi Y, Xu L, Shi Y, Li C (2018) Experimental Investigation on the flexural behavior of steel-polypropylene hybrid fiber reinforced concrete. Constr Build Mater 191:80–94

Lim TY, Paramasivam P, Lee SL (1987), "Analytical model for tensile behavior of steel-fiber concrete", ACI Mater J, 84(4)

Naaman AE, Reinhardt HW (2006) Proposed classification of HPFRC composites based on their tensile response. Mater Struct 39(5):547

Neville AM, Brooks JJ (2010), "Concrete technology", Longman Scientific & Technical

Nuruddin MF, Khan SU, Shafiq N, Ayub T (2014), "Strength development of high-strength ductile concrete incorporating metakaolin and Pva fibers", The Sci World J, 2014

Parameswaran VS (1991) Fibre-reinforced concrete: a versatile construction material. Build Environ 26(3):301–305

Peyvandi A, Soroushian P, Jahangirnejad S (2013) Enhancement of the structural efficiency and performance of concrete pipes through fiber reinforcement. Constr Build Mater 45:36–44

Qian C, Stroeven P (2000) Development of hybrid polypropylene-steel fibre-reinforced concrete. Cem Concr Res 30(1):63–69

Said M, Abd El-Azim AA, Ali, MM, El-Ghazaly H, Shaaban I (2020), "Effect of elevated temperature on axially and eccentrically loaded columns containing polyvinyl alcohol (Pva) fibers", Eng Struct 204: 110065

Shah SP, Daniel JI, Ahmad SH, Arockiasamy M, Balaguru P, Ball CG, Ball HP Jr, Banthia N, Batson GB, Bentur A (1993) Guide for specifying, proportioning, mixing, placing, and finishing steel fiber reinforced concrete. ACI Mater j 90(1):94–101

Shi F, Pham TM, Hao H, Hao Y (2020), Post-Cracking Behaviour of Basalt and Macro Polypropylene Hybrid Fibre Reinforced Concrete with Different Compressive Strengths, Constr Build Mater, 262: 120108

Sivakumar A, Santhanam M (2007) Mechanical properties of high strength concrete reinforced with metallic and non-metallic fibres. Cement Concr Compos 29(8):603–608

Soe KT, Zhang Y, Zhang L (2013) Material properties of a new hybrid fibre-reinforced engineered cementitious composite. Constr Build Mater 43:399–407

Song P, Wu J, Hwang S, Sheu B (2005) Statistical analysis of impact strength and strength reliability of steel-polypropylene hybrid fiber-reinforced concrete. Constr Build Mater 19(1):1–9

Sukontasukkul P (2004) Tensile behaviour of hybrid fibre-reinforced concrete. Adv Cem Res 16(3):115–122

Tabatabaeian M, Khaloo A, Joshaghani A, Hajibandeh E (2017) Experimental investigation on effects of hybrid fibers on rheological, mechanical, and durability properties of high-strength SCC. Constr Build Mater 147:497–509

Tian H, Zhang Y, Ye L, Yang C (2015) Mechanical behaviours of green hybrid fibre-reinforced cementitious composites. Constr Build Mater 95:152–163

Wang S, Li VC (2003), "Tailoring of Pva fiber/matrix interface for engineered cementitious composites (ECC)"

Xiaochun Q, Xiaoming L, Xiaopei C (2017) The applicability of alkaline-resistant glass fiber in cement mortar of road pavement: corrosion mechanism and performance analysis. Int J Pavement Res Technol 10(6):536–544

Yokota H, Rokugo K, Sakata N (2008) JSCE recommendations for design and construction of high performance fiber reinforced cement composite with multiple fine cracks. In: High performance fiber reinforced cement composites. Springer, Tokyo, Japan

Yildizel SA, Tayeh BA, Calis G (2020) Experimental and modelling study of mixture design optimisation of glass fibre-reinforced concrete with combined utilisation of Taguchi and extreme vertices design techniques. J Market Res 9(2):2093–2106

Zeyad AM, Khan AH, Tayeh BA (2020) Durability and strength characteristics of high-strength concrete incorporated with volcanic pumice powder and polypropylene fibers. J Market Res 9(1):806–818

Zheng Z, Feldman D (1995) Synthetic fibre-reinforced concrete. Prog Polym Sci 20(2):185–210